Numerical evaluation of path-integral solutions to Fokker-Planck equations

M. F. Wehner and W. G. Wolfer
Fusion Engineering Program, Nuclear Engineering Department,
University of Wisconsin, Madison, Wisconsin 53706
(Received 15 November 1982)

A numerical method, based on the path-integral formalism, is presented to solve nonlinear Fokker-Planck equations with natural boundary conditions. For one-dimensional stochastic processes, several specific examples possessing exact analytic solutions are evaluated numerically for purposes of comparison. Various discretization prescriptions are investigated and found to be equivalent as expected. The numerical method is shown to give accurate results provided the spatial discretization and the time step satisfy certain relationships determined by the drift and the diffusion functions of the nonlinear Fokker-Planck equations.

I. INTRODUCTION

Significant advances have been made in recent years towards a general theory of macroscopic systems far from a thermodynamic equilibrium state. Many of these systems, as pointed out by Graham,[1] Haken,[2] Nicolis and Prigogine,[3] Schenzle and Brand,[4] and many others, can be described by nonlinear Fokker-Planck equations. The term "nonlinear" refers in the present context to the nonlinear dependence of the drift vector and of the diffusion tensor on the state variables q_i $(i=1,2,\ldots,n)$ which characterize the macroscopic state of the system. In reality, the nonlinear Fokker-Planck equation is a linear partial differential equation of second order and of the parabolic type.

This equation is the prototype of an evolution equation which describes both the deterministic path of the system as determined by the drift vector as well as fluctuations away from this path as determined by the diffusion tensor. As a result of these fluctuations, the state of the system can be specified only by a probability density

$$P(q_1,q_2,\ldots,q_n,t)\ ,$$

where this distribution function P satisfies the nonlinear Fokker-Planck equation

$$\frac{\partial P}{\partial t}=-\frac{\partial}{\partial q_i}\left[K_i-\frac{1}{2}\frac{\partial}{\partial q_j}Q_{ij}\right]P \tag{1}$$

together with appropriate boundary conditions. Here, $K_i(\vec{q})$ is the aforementioned drift vector, $\frac{1}{2}Q_{ij}(\vec{q})$ the diffusion tensor, and repeated indices imply a summation.

This equation is exactly solvable only for specific choices of the drift vector and the diffusion tensor. Cukier *et al.*[5] have discussed cases where the Fokker-Planck equation can be solved with the classical orthogonal polynomials. Schenzle and Brand[4] have investigated the conditions for which the eigenfunction expansion can be utilized as a method of solution. For this to be possible, the Fokker-Planck equation must be transformed into a self-adjoint equation.

Of course, it is always possible to employ existing methods for numerical solution, such as finite-difference methods.[6,7] However, these methods often lead to stiff systems of ordinary differential equations in the time variable. Like chemical rate equations, their long-term numerical integration requires excessive computer time.[8] If information is needed only about certain properties of the system without direct reference to the probability density $P(\vec{q},t)$ the mathematically equivalent stochastic differential equation may be numerically integrated by Monte Carlo techniques.[9]

In recent years a major effort has been devoted to derive a formal solution of the nonlinear Fokker-Planck equation in terms of a path integral.[2,10–18] The particular interest in such a formulation originates from various considerations. The path integral can provide a convenient starting point for approximate solutions centered around the deterministic path. Also, analogies can be drawn between quantum mechanics and nonequilibrium thermodynamics to shed further light on the latter.[19] And then, perhaps most importantly, the path integral appears to provide a formalism which allows the extension of the thermodynamic equilibrium concepts, such as entropy and thermodynamic potentials into

the domain of nonequilibrium thermodynamics.[16,18,20]

In this formalism, the solution of Eq. (1) is written in terms of a functional integral, i.e.,

$$P(q,t)=\int_{q_0}^{q} D\mu(q)\exp\left[-\int_{t_0}^{t}\mathscr{L}(\dot{q}(t'),q(t'))dt'\right]P(q_0,t_0)\ . \tag{2}$$

Here, $D\mu(q)$ is an integration measure and $\mathscr{L}$ is often referred to as the Onsager-Machlup functional. Much of the confusion involving path integrals stems from the fact that the many derivations in the literature, although all equally valid, do not and cannot uniquely specify the Onsager-Machlup functional. The issues are further complicated by the requirement that Eq. (2) be of a covariant form, i.e., that the Onsager-Machlup functional transforms according to the usual rules of calculus when a nonlinear point transformation is made in the state space.[13,14] This property is necessary if a consistent theory of nonequilibrium thermodynamics is to be based on the path integral.

The simplest approach to define the path integral starts by representing the continuous process in the limit of infinitesimally spaced lattice points in space and time. However, because there exists no unique discrete representation of a continuous process, many different path integrals corresponding to various discretization prescriptions have resulted.[11,15,17] To construct in this manner a path integral which is covariant requires a specific *a priori* choice of the discretization procedure. This had led other authors to present different methods of deriving a covariant path integral without assuming an *ad hoc* discretization rule.[13,14,16] A discrete lattice representation can then be chosen afterwards, if so desired.

In actual practice, in spite of the elegance and conceptual value of the path integral, the evaluation of Eq. (2), whether analytical or numerical, has not been possible in the general case. It is the main purpose of this and future papers to remove this limitation by developing numerical methods based on the discrete equivalent to Eq. (2). In the present paper, we present such a method for one-dimensional ($n=1$) unrestricted stochastic processes with natural boundary conditions.

In Sec. II, the discrete path sum is reviewed and the selection of a discretization rule is discussed. In Sec. III, we describe the numerical procedure developed for the evaluation of the path sum. In Sec. IV, specific examples, possessing closed-form analytic solutions are evaluated numerically in order that the accuracy of the method may be tested. Finally, we discuss the present approach and its possible extensions in Sec. V.

II. PATH SUM

Our point of departure is the path sum or discrete lattice representation of the path integral. This has been the traditional approach to define the path integral but, as previously mentioned, does not always lead to uniquely covariant forms. However, since the purpose of this paper is to find solutions of Eq. (1) rather than to seek thermodynamic interpretations, the path sum forms an adequate and flexible basis for a numerical scheme.

In its usual form the path sum is written as

$$P(q,t)=\lim_{\substack{\tau\to 0\\ N\to\infty\\ N\tau\to t-t_0}}\prod_{i=0}^{N-1}\int\cdots\int(\mu_i dq_i)\exp\left[-\tau\sum_{j=0}^{N-1}\mathscr{L}(q_{j+1},q_j,\tau)\right]P(q_0,t_0)\ , \tag{3}$$

where

$$G(q_{i+1},q_i,\tau)=\mu_i\exp[-\tau\mathscr{L}(q_{i+1},q_i,\tau)]$$

is often referred to as the short-time propagator. The many possible discretization rules lead to the different forms of G. The only requirement made on the propagator is that it satisfy Eq. (1) to order $O(\tau^2)$. Our primary focus then becomes determining which path sum formulation yields the most accurate and concise numerical procedure. A particularly simple, yet illustrative choice is[15]

$$G(q,q',\tau)=(2\pi\tau)^{-n/2}||\bar{Q}||^{-1/2}\exp\left[-\frac{\tau}{2}\left[-aQ_{\nu\lambda}^{(\lambda)}(q)+\bar{K}_\nu-\frac{(q_\nu-q'_\nu)}{\tau}\right]\right.$$
$$\left.\times(\bar{Q}_{\nu\mu})^{-1}\left[-aQ_{\mu\rho}^{(\rho)}(q)+\bar{K}_\mu-\frac{(q_\mu-q'_\mu)}{\tau}\right]-\frac{a}{2}Q_{\nu\mu}^{(\nu\mu)}(q)+aK_\nu^{(\nu)}(q)\right]\ , \tag{4}$$

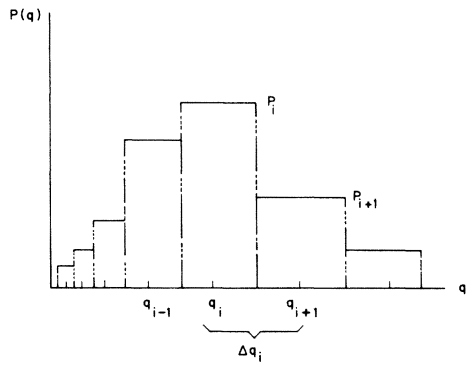

FIG. 1. Histogram representation of the distribution function.

where

$$\bar{Q}=aQ(q)+bQ(q')\ ,$$
$$\bar{K}=aK(q)+bK(q')\ ,$$

and

$$a+b=1,\quad 0\le a,b\le 1\ .$$

The subscript is the tensor (or vector) index and the superscripts denote differentiation.

This function defines a class of propagators determined by the choices of a and b. These parameters establish the discretization rule by evaluating the Fokker-Planck coefficients at a linear combination of postpoint and prepoint. The effect of this feature on the numerical procedure is discussed via a specific example in Sec. IV A.

III. NUMERICAL PROCEDURE

The numerical scheme to solve the Fokker-Planck equation is based on the iterative nature of Eq. (3). In one dimension, for a single iteration, Eq. (3) becomes

$$P(q,t+\tau)=\int dq'G(q,q',\tau)P(q',t)\ . \tag{5}$$

We assume that the probability distribution can be represented with sufficient accuracy by a histogram as given by

$$P(q,t)=\sum_{i=1}^{N}\pi(q-q_i)P_i(t)$$

and as shown schematically in Fig. 1. Here

$$\pi(q-q_i)=\begin{cases}1 & \text{for } q_i-\frac{1}{2}\Delta q_{i-1}\le q\le q_i+\frac{1}{2}\Delta q_i\ ,\\ 0 & \text{otherwise}\ .\end{cases}$$

The index i is not to be confused with the indices in Eqs. (3) or (4). After substitution of the histogram representation into Eq. (5), we integrate over the interval centered at the grid point q_i and divide the integral over dq' into N parts to obtain

$$P_i(t+\tau)=\sum_{j=1}^{N}T_{ij}(\tau)P_j(t)\ , \tag{6}$$

where we have defined the propagator matrix as

$$T_{ij}(\tau)=\frac{2}{\Delta q_{i-1}+\Delta q_i}\int_{q_i-\Delta q_{i-1}/2}^{q_i+\Delta q_i/2}dq\int_{q_j-\Delta q_{j-1}/2}^{q_j+\Delta q_j/2}dq'G(q,q',\tau)\ . \tag{7}$$

This equation is in a form suitable for programming. The integrations in (7) need only be performed once for a given time step τ and can then be stored and used repeatedly to compute the time evolution of the histogram via Eq. (6). In the limit $\tau\to 0$, the propagator matrix degenerates into the unity matrix δ_{ij}. This implies that for small but nonzero time steps, the propagator matrix is banded with off-diagonal elements decreasing rapidly in magnitude with increasing distance from the diagonal. The width of this band of significant elements increases with increasing τ. This banded structure of T_{ij} implies that much fewer than N^2 elements need to be computed and stored; thus the operations involved in Eq. (6) require much less computer time and memory. For a general choice of a and b in Eq. (4), both integrations must be performed numerically. We shall return to this point in Sec. IV.

The choice of the time step τ and the interval sizes Δq_i are intimately connected to the stochastic nature of the process under consideration. We may view the histogram $P_i(t)$ as an approximation for a superposition of Gaussian distributions centered around the grid points. After the time τ, these distributions broaden and, if subject to a drift force, shift. For a point initially located at q_i, the first and second moments are given as[21]

$$\langle q-q_i\rangle=K(q_i)\tau+\cdots\ , \tag{8}$$
$$\langle(q-q_i)^2\rangle=Q(q_i)\tau+\cdots\ ,$$

where the ellipses denote unspecified higher-order terms.

The second moment may be interpreted as a characteristic width or standard deviation of the process while the first moment is equivalent to an

average displacement. To determine a condition on the value of τ, we require that the random nature of the process be a greater influence than the deterministic forces. More precisely, we require that the average displacement of a "particle" at q_i be less than the "width" of the corresponding relaxed distribution after the time τ. From Eq. (8), it is apparent that

$$0<\tau<\frac{Q(q)}{[K(q)]^2} . \tag{9}$$

By requiring this relation to hold over the entire region of q where $P(q,t)$ has an appreciable value, a condition on the magnitude of τ is provided.

The second moment may further be interpreted as a width in connection with the choice of the grid spacing. In all of the cases tested in Sec. IV, the relation

$$\Delta q_i=[Q(q_i)\tau]^{1/2} \tag{10}$$

had to be satisfied in order to obtain correct results. The grid points q_i are located with spacing Δq_i as in Fig. 1. This equality is in contrast to other numerical methods of solving diffusion equations where greater accuracy is obtained by choosing smaller time steps than dictated by Eq. (10).[22] This scaling of the interval spacing by both the diffusion coefficient and the time step was found to be essential to the numerical stability of the routine. A deviation from the equality in Eq. (10) by as little as 10 percent adversely affects the accuracy of the numerical results.

There are several causes which can lead to numerical error propagation. These effects can be minimized by taking advantage of the normalizability of both the distribution function and of the propagator function. If the bandedness of the propagator matrix is used to reduce computer time, error may be introduced by the selection of too narrow a band. To reduce this source of error, we note that

$$\int dq\, G(q,q',\tau)=\sum_i \int_{q_i-\Delta q_{i-1}/2}^{q_i+\Delta q_i/2} dq\, G(q,q',\tau)$$

$$=1 .$$

From the definition of the propagator matrix (7) we see that

$$\sum_i T_{ij}(\tau)\frac{(\Delta q_i+\Delta q_{i-1})}{2}=\int_{q_j-\Delta q_{j-1}/2}^{q_j+\Delta q_j/2} dq'$$

$$=\frac{\Delta q_j+\Delta q_{j-1}}{2} .$$

If, after the numerical integration

$$\sum_i T_{ij}(\tau)\frac{(\Delta q_i+\Delta q_{i-1})}{2}=\left[\frac{\Delta q_j+\Delta q_{j-1}}{2}\right]A_j ,$$

we make the transformation

$$T_{ij}^{\text{new}}\rightarrow\frac{T_{ij}^{\text{old}}}{A_j} , \tag{11a}$$

the normalization of the propagator matrix is assured.

Similarly, truncation error can also be introduced through the evaluation of the sum in Eq. (6). To reduce this type of error, the sum

$$\sum_i P_i(t)\Delta q_i=1+\epsilon$$

is determined. The exact probability distribution, when integrated over q, would of course result in unity. Therefore, the discrete representation is renormalized to

$$P_i(t)=\frac{1}{1+\epsilon}P_i(t) \tag{11b}$$

before being used again in the right-hand side of Eq. (8) for the next iteration. It was found that these conservation properties of the zeroth moments of the probability and propagator functions could significantly increase the accuracy of the numerical method, especially for long-time cases.

IV. RESULTS

In order to test the usefulness, accuracy, and limitations of this numerical path sum method, various Fokker-Planck equations were solved using the above method, and they were then compared to the exact analytical solutions known for these cases. For examples presented here, the initial conditions were specified as the usual delta function $\delta(q-q_0)$. As an approximation in the numerical method, we represented the δ function by a single histogram element where the height of the element was equal to the reciprocal of the width. Both the Wiener process (constant coefficients) and the Ornstein-Uhlenbeck process (linear drift) were tested with very good results. However, since these path integrals may be done exactly, we pass over to more complicated nonlinear problems.

One question of interest arising from the choice of Eq. (4) as the propagator concerns the values of a and b. These parameters determine the discretization rule by representing the Fokker-Planck coefficients as a linear combination around the postpoints and prepoints. To determine if an optimal combination exists, a problem must be chosen which possesses a nonvanishing second derivative of the

diffusion coefficient in order that all the terms in Eq. (4) are represented. To find such a problem with a known solution (for purposes of comparison), we take advantage of a technique due to Haken[11] and Hänggi.[23]

A. Transformed Ornstein-Uhlenbeck process

By introducing a suitable coordinate transformation, we may obtain from the Ornstein-Uhlenbeck (OU) process a whole class of Fokker-Planck equations with exact solutions. An OU process is characterized by

$$K(x)=\alpha x+\beta$$

and

$$Q=\text{const}.$$

Introducing the transformation

$$x=F(q) \tag{12}$$

implies that

$$p(x,t)=H(q)h(q,t)\ , \tag{13}$$

where p and h are the probability distributions corresponding to x and q, respectively, and

$$F'(q)=dF/dq=H^{-1}(q)\ .$$

Then the Fokker-Planck equation in the transformed space becomes[11]

$$\frac{\partial h(q,t)}{\partial t}=-\frac{\partial}{\partial q}\left[\left[[\alpha F(q)+\beta]H(q)+\frac{Q}{2}H'H\right]h(q,t)+\frac{Q}{2}\frac{\partial^2}{\partial q^2}[H^2h(q,t)]\right]\ . \tag{14}$$

The solution to this equation is determined by the solution to the Ornstein-Uhlenbeck process along with Eqs. (12) and (13).

As a particular example to satisfy our needs, let

$$x=F(q)=\ln[q+(q^2+a^2)^{1/2}]\ ; \tag{15}$$

then H becomes

$$H(q)=(q^2+a^2)^{1/2}\ . \tag{16}$$

If we let $\alpha=0$, $\beta=1$, $a=1$, and $Q=1$, we find that the transformed Fokker-Planck coefficients are

$$K(q)=(q^2+1^2)^{1/2}+q/2 \tag{17}$$

and

$$Q(q)=q^2+1\ .$$

The solution for an initial δ distribution is

$$h(q,t)=f(q,t)/(q^2+1)^{1/2}\ , \tag{18}$$

where f is defined by the Wiener solution

$$f(q,t)=\frac{1}{\sqrt{2Q\pi t}}\times\exp\left[\frac{-[F(q)-F(q_0)-\beta t]^2}{2Qt}\right]\ ,$$

together with the transformation given by Eq. (15). This problem allows for a thorough test of the propagator as defined in Eq. (4).

We evaluated the Fokker-Planck coefficients Eq. (17) at a variety of linear combinations of postpoints and prepoints. It was found that very little change in numerical accuracy was obtained for differing values of a and b. This fact leads to a great simplification in the technique. If we choose $a=0$ in Eq.

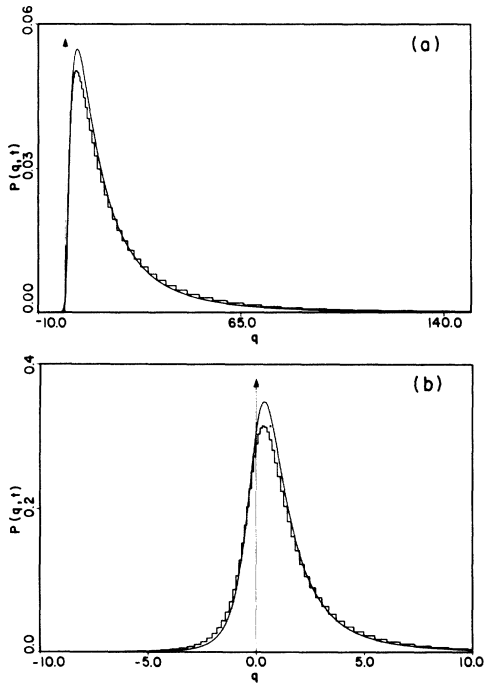

FIG. 2. (a) Wiener process subject to the transformation $x=F(q)=\ln[q+(q^2+1)]^{1/2}$. The time is 1.0 and the time step is chosen as 0.01. Initial δ function at $q_0=4.3$. (b) Wiener process subject to the transformation $x=F(q)=\ln[q+(q^2+1)^{1/2}]$. The time is 1.0 and the time step is chosen as 0.01. Initial δ function at $q_0=-0.25$.

(4), the exponent in the propagator becomes a simple quadratic function of the postpoint and the integration in Eq. (7) over the postpoint may be performed in a closed form. The remaining integral over the prepoint is done numerically with greater accuracy and less effort. Figures 2(a) and 2(b) show the accuracy of the histogram compared to the exact solution for two different initial conditions. The shape of the curve is strongly dependent on the choice of the initial condition. In Fig. 2(a), the drift coefficient is large compared to the diffusion coefficient and positive at the position of the initial δ function; hence the steep rise to the right of the δ function.

B. The Rayleigh gas

The Rayleigh gas is a model system consisting of a dilute concentration of heavy atoms in a gas of light atoms.[24] Assuming hard-sphere collisions, the Boltzmann collision equation can be reduced to a Fokker-Planck equation for the energy spectrum of the heavy particles. This equation has a drift function of

$$K=-q+\tfrac{3}{2} \tag{19a}$$

and a diffusion function of

$$Q=2q\ . \tag{19b}$$

Since the particle energy can only be positive, this Fokker-Planck equation is valid for the domain $0\le q<\infty$. The boundary at zero is referred to as an inaccessible natural boundary.

When the initial energy distribution of the heavy particles is a δ function $\delta(q-q_0)$, the distribution function is given by[24]

$$P(q,t)=\frac{e^{t/2}}{2[\pi q_0(1-e^{-t})]^{1/2}}\left[\exp\left[-\frac{[q^{1/2}-(q_0e^{-t})^{1/2}]^2}{1-e^{-t}}\right]-\exp\left[-\frac{[q^{1/2}+(q_0e^{-t})^{1/2}]^2}{1-e^{-t}}\right]\right]. \tag{20}$$

The type of boundary involved in the Rayleigh gas model points out one of the limitations of the numerical path sum. As q approaches zero, the diffusion coefficient vanishes, resulting in a completely deterministic process. Yet the boundary is a natural one since the drift force is repulsive at $q=0$, forcing the energy to maintain a positive value. No other boundary conditions need be explicitly specified.[25] This loss of stochasticity at $q=0$ is inconsistent with a path-integral formulation. If the distribution function has evolved to the point where it has an appreciable value very close to zero, the numerical results tend to be in error. This also becomes apparent in the choice of the time step τ. From Eq. (9), it is seen that the inequality

$$\tau<\frac{Q(q)}{K^2(q)}=\frac{2q}{(q-\frac{3}{2})^2}$$

cannot be satisfied by a nonzero value of τ over the entire domain. The development of the distribution is shown in Figs. 3(a) and 3(b). Here τ was chosen as 0.01 which defines the valid domain as $0.011<q<200$. In Fig. 3(b) the distribution has evolved to the extent where its value is significant outside this domain. Hence, the above inequality for τ is no longer satisfied for $q<0.011$, and the distribution function is expected to be in error. Owing to the normalization procedure, this error is then spread over the entire range where the distribution function assumes significant values.

C. Stochastic processes with bifurcation

Recently, two separate classes of nonlinear Fokker-Planck equations with bifurcating solutions

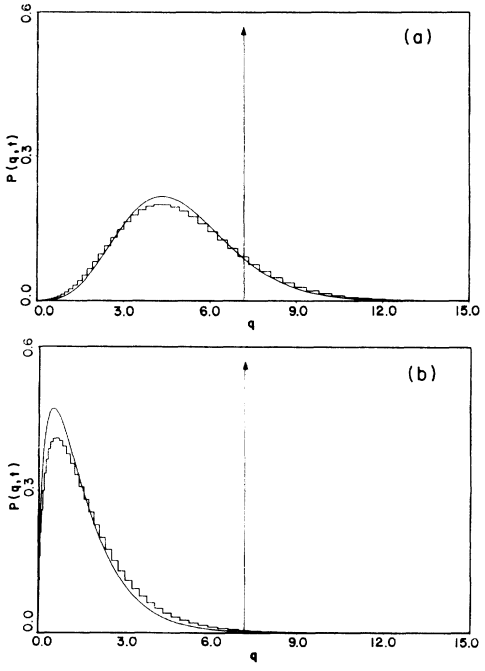

FIG. 3. (a) Rayleigh gas subject to initial condition at $q_0=7$. The time step is chosen as 0.01. Time equals 0.5. (b) Rayleigh gas subject to initial condition at $q_0=7$. The time step is chosen as 0.01. Time equals 5.0; at this point the process has reached its equilibrium distribution.

appeared in the literature.[19,26] This type of distribution function is characterized by multiple maxima and tend to be intrinsically non-Gaussian. One of these processes has a steady-state solution independent of the initial condition. The other, however, has no steady-state solution, and the distribution function always depends on the initial condition. It is of particular interest to know if the numerical path sum will accurately reproduce a bifurcating solution since none of that information is contained in the short-time propagator G, but only in the Fokker-Planck coefficients themselves.

The first type of equation is characterized by the drift force

$$K(q)=\tanh q \tag{21}$$

and a constant diffusion coefficient. For $Q=1$, the time-dependent solution subject to an initial δ-function distribution at q_0 is[26]

$$P(q,t)=[\mathrm{sech}(q_0)/(2\pi t)^{1/2}]\exp(-t/2)\exp[-(1/2t)(q-q_0)^2]\cosh q\ . \tag{22}$$

This distribution is actually a superposition of two Gaussians and has no nonzero steady state. In Figs. 4(a) and 4(b) we show the numerical and analytical solutions at time $t=10$ for two different initial δ functions at $q_0=0$ and $q_0=0.6$. The relative size of the two peaks depends critically on the initial position of the δ function.

A second class of bifurcating processes which do possess a nontrivial steady state is characterized by

$$K(q)=-\tfrac{1}{4}\tanh q-\frac{1}{2}\frac{\tanh q}{\cosh^2 q} \tag{23a}$$

and

$$Q(q)=(\cosh q)^{-2}\ . \tag{23b}$$

The solution subject to an initial δ function at q_0 is given by[19]

$$P(q,t)=[4\pi(1-z^2)]^{-1/2}\cosh(q)\exp\{-[4(1-z^2)]^{-1}(\sinh q-z\sinh q_0)^2\}\ , \tag{24}$$

where $z=e^{-t/4}$.

Figure 5 shows the analytical and numerical solutions for the steady-state reached by this process. It is important to note that of the several different initial conditions investigated, all resulted in the same numerical steady-state solution.

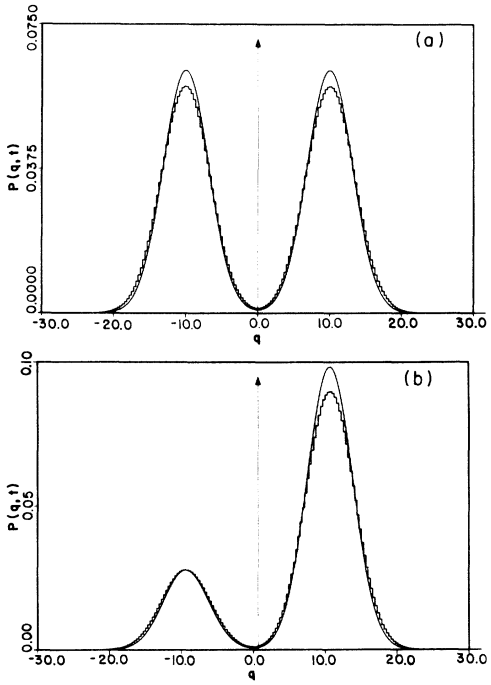

FIG. 4. (a) The process defined by a drift force $K=\tanh q$ and constant diffusion at time $t=10$. The time step is chosen as 0.1. Initial condition at $q_0=0$. Note that the distribution is symmetric. (b) The process defined by a drift force $K=\tanh q$ and constant diffusion at time $t=10$. The time step is chosen as 0.1. Initial condition at $q_0=0.6$. A small displacement of the initial condition from the position $q_0=0$ results in an asymmetric distribution.

V. CONCLUSION

Starting from the discrete equivalent to the path integral, we have presented an efficient numerical method to solve nonlinear Fokker-Planck equations. In Sec. IV, we saw that the numerical results are generally in good agreement with the analytic solutions. From Figs. 2–5, certain qualitative observa-

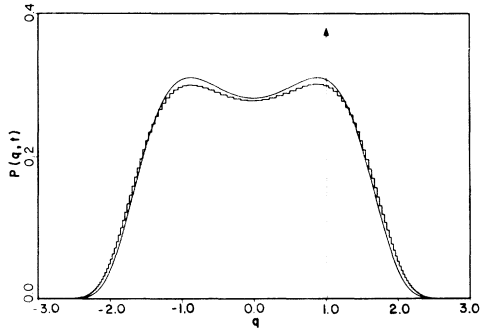

FIG. 5. The equilibrium distribution for the process defined by Eq. (27). This distribution was reached numerically from a variety of initial conditions.

tions can be made regarding the relative accuracy of the numerical results. Typically, the numerical method predicts a peak which is too low by a few percent. The results in the "wings" of the distribution are therefore somewhat higher because of the normalization condition. After a certain point, this discrepancy cannot be further reduced by choosing smaller time intervals. This contradicts what would be expected from the mathematical path-integral definition as a limit of path sums of infinitesimally small time steps. The inaccuracies must then arise from the assumptions made to develop the numerical method. A possible explanation is that the histogram (being composed only of horizontal and vertical elements) fails to describe regions of high curvature. Examining Fig. 2(a), we note that the agreement to the far right of the peak is quite good. Similarly, the extremely steep portion of the curve is also matched well. Both of these regions are of relatively low curvature as compared to the region near the peak. An improvement on the histogram would be a trapezoidal (or some curved) relation between the points, P_i. This is analogous to the various approximations to the Riemannian integral. Overall, however, given the crude assumptions of the histogram, the values and shapes of the curves are reproduced well.

A specific practical advantage of a path-integral-based numerical method is the efficiency in terms of computer time. Once the integrations in Eq. (7) are performed and stored, the time evolution of the histogram can be obtained simply by a sequence of multiplications. With today's high-speed computers such sequences are very rapidly executed. The extension to an n-dimensional problem would simply entail n numerical integrations, assuming the simplest choice of the propagator function.

Another important point is the fundamental physical significance of the path integral as opposed to other procedures (e.g., finite differences) for a numerical method to solve Eq. (1). The assumption that for small time intervals the relaxation is Gaussian is an underlying consequence of the general nonlinear Fokker-Planck equation. As the examples in Sec. IV have shown, this property can be used to develop non-Gaussian distributions for longer time intervals.

We believe that the present numerical method can be used as a practical tool for solving most nonlinear Fokker-Planck equations. One additional complication arises for stochastic processes which require in addition to Eq. (1) the specification of external boundary conditions (i.e., boundaries not naturally contained in the Fokker-Planck coefficients themselves). In a future paper, we will expand the path sum formalism and our numerical procedure to deal with external boundary conditions.

ACKNOWLEDGMENTS

This research was supported by the U.S. Department of Energy under Contracts Nos. ER-78-S-02-4861 and DE-AC02-82ER52082 at the University of Wisconsin.

[1]R. Graham, Springer Tracts Mod. Phys. 66, 1 (1973).
[2]H. Haken, Rev. Mod. Phys. 47, 175 (1975); *Synergetics,* 2nd ed. (Springer, Berlin, 1978).
[3]G. Nicolis and I. Prigogine, *Self-Organization in Non-Equilibrium Systems* (Wiley-Interscience, New York, 1977).
[4]A. Schenzle and H. Brand, Phys. Rev. A 20, 1628 (1979).
[5]R. I. Cukier, K. Lakatos-Lindenberg, and K. E. Shuler, J. Stat. Phys. 9, 137 (1973).
[6]G. D. Smith, *Numerical Solution of Partial Differential Equations* (Oxford University Press, New York, 1965).
[7]G. E. Forsythe and W. R. Wasow, *Finite Difference Methods for Partial Differential Equations* (Wiley, New York, 1967).
[8]A. C. Damask and G. Dienes, Phys. Rev. 120, 99 (1960).
[9]D. L. Ermak and H. Buckholtz, J. Comp. Phys. 35, 169 (1980).
[10]W. Horsthemke and A. Bach, Z. Phys. B 22, 189 (1975).
[11]H. Haken, Z. Phys. B 24, 321 (1976).
[12]R. Graham, Z. Phys. B 26, 281 (1976).
[13]H. Dekker, Physica (Utrecht) 85A, 363 (1976); Phys. Rev. A 19, 2102 (1979).
[14]U. Deininghaus and R. Graham, Z. Phys. B 34, 211 (1979).
[15]C. Wissel, Z. Phys. B 35, 185 (1979).
[16]H. Grabert and M. S. Green, Phys. Rev. A 19, 1747 (1979).
[17]F. Langouche, D. Roekaerts, and E. Tirapegui, Nuovo Cimento B 53, 135 (1979).
[18]H. Grabert, R. Graham, and M. S. Green, Phys. Rev. A 21, 2136 (1980).
[19]J-C. Zambrini and K. Yasue, Ann. Phys. (N.Y.) 125, 176 (1980).
[20]R. Graham, in *Functional Integration, Theory and Applications,* edited by J-P. Antoine and E. Tirapegui (Plenum, New York, 1980).
[21]L. Arnold, *Stochastic Differential Equations: Theory and Applications* (Wiley-Interscience, New York, 1974).
[22]H. S. Carslaw and J. C. Jaeger, *Conduction of Heat in Solids* (Oxford University Press, London, 1959).
[23]P. Hänggi, Z. Phys. B 30, 85 (1978).
[24]K. Anderson and K. E. Shuler, J. Chem. Phys. 40, 633 (1964).
[25]P. Hänggi, K. Shuler, and I. Oppenheim, Physica (Utrecht) 107A, 143 (1981).
[26]M. O. Hongler, Phys. Lett. 75A, 3 (1979).